

CrystEngComm

Accepted Manuscript



This is an *Accepted Manuscript*, which has been through the Royal Society of Chemistry peer review process and has been accepted for publication.

Accepted Manuscripts are published online shortly after acceptance, before technical editing, formatting and proof reading. Using this free service, authors can make their results available to the community, in citable form, before we publish the edited article. We will replace this *Accepted Manuscript* with the edited and formatted *Advance Article* as soon as it is available.

You can find more information about *Accepted Manuscripts* in the [Information for Authors](#).

Please note that technical editing may introduce minor changes to the text and/or graphics, which may alter content. The journal's standard [Terms & Conditions](#) and the [Ethical guidelines](#) still apply. In no event shall the Royal Society of Chemistry be held responsible for any errors or omissions in this *Accepted Manuscript* or any consequences arising from the use of any information it contains.



Journal Name

COMMUNICATION

Supramolecular interactions in boron hydrides: How non-classical bonding directs their crystal architecture

Received 00th January 20xx,
Accepted 00th January 20xx

David J. Wolstenholme,^{a,*} Eric J. Fradsham^a and G. Sean McGrady^{a,*}

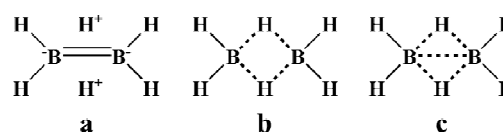
DOI: 10.1039/x0xx00000x

www.rsc.org/

Boron hydrides typically contain both bridging B-H-B and terminal B-H bonds, which behave respectively as local Lewis acidic and basic sites. Their condensed phases are then stabilised through dihydrogen bonds between these hydride moieties. Here we explore the complex interplay of these H...H interactions for simple boranes, and we discuss the influence of 3c,2e B-H-B and B-B-B bonding on their extended structures. This analysis has also revealed a novel form of heteropolar dihydrogen bonding, involving an acidic B-H-B bridging and a basic terminal B-H moiety.

The hydrides of boron have played a central role in the development of synthetic and theoretical inorganic chemistry for almost a century. Their discovery by Stock in the early 1930's provoked considerable debate regarding the structure and bonding of these remarkable molecules.¹⁻⁵ This led Pitzer et al. to propose a model for diborane-6 (B_2H_6 - **1**) that closely resembles its isoelectronic ethene counterpart, with a doubly protonated $[H_2B=BH_2]^{2-}$ framework (Scheme 1a).² However, the 1H NMR spectrum of liquid **1** revealed that the bridging hydrogen atoms are negatively charged, consonant with an alternative "three-centre, two-electron" (3c,2e) bonding motif (Scheme 1b).³ This concept was further supported by MO theory, with the electrons located in B-H-B bonding orbitals being distributed evenly across these moieties.⁴ Subsequently, the structure of **1** was proposed to involve an electron-deficient B...B interaction (Scheme 1c), implying hybrid σ - and π -type character for this bond.⁵ These studies serve to rationalise the non-classical bonding in **1** and related boranes, but they fail to describe how these structural motifs influence the supramolecular interactions responsible for stabilising the condensed phases of these systems.

In the solid state, the bridging and terminal hydrogen atoms of boranes may be expected to engage in distinct types of intermolecular H...H interactions that contribute to their crystalline



Scheme 1. Alternative bonding motifs for diborane **1**.

architecture. For example, the neo-conventional 3c,2e bonding motif **1b** would allow the B_2H_6 molecules to engage in counter-intuitive hydride-hydride bonding.⁶ Therefore, as an extension of our recent programme directed at understanding these and related H...H interactions, we have revisited the molecular and electronic structures of a series of simple boranes (B_2H_6 , B_4H_{10} , B_5H_9 , and $B_{10}H_{14}$), along with exploring the influence of 3c,2e B-B-B and B-H-B bonding in directing these supramolecular interactions.⁶ These compounds offer a rare opportunity to analyse weak dihydrogen bonding free from any competing interactions, and as such they afford a unique insight into the nature and the driving forces behind the formation of these unconventional H...H interactions.

Crystalline **1** adopts the monoclinic space group $P2_1/n$ (#14), in which the body-centred orientation of the molecules gives rise to discrete B_2H_6 fragments that form several H...H contacts below the sum of the van der Waals radii for two interacting hydride ions ($< 2.8 \text{ \AA}$).^{6,7} This prompted us to explore in detail the charge distribution in **1**, since no competing interactions are present to interfere with the dihydrogen bonding. In this instance, the electrostatic potential mapped onto a 0.001 au isodensity surface revealed a significant electrophilic region surrounding the bridging hydrogen atoms, with the most nucleophilic portions of the molecule being located between the terminal B-H moieties (Fig. 1). This redistribution of charge is most consistent with the doubly-protonated $[H_2B=BH_2]^{2-}$ model **1a**, and suggests that the condensed phase of **1** is stabilised through B-H...H-B proton-hydride interactions. Similar behaviour has been predicted computationally for B_2H_6 interacting with basic molecules (e.g. CH_3OH), with the bridging hydrogen atoms acting as hydrogen-bond donors.⁸ However, closer inspection of the MOs that contribute to the $B(\mu-H)_2B$ region clearly reveals delocalisation throughout this moiety, consonant with the widely accepted 3c,2e bonding motif.

^a Department of Chemistry, University of New Brunswick, P.O. Box 4400, Fredericton, N.B., Canada, E3B 5A3, e-mail: dwolsten@unb.ca and smcgrady@unb.ca.

Electronic Supplementary Information (ESI) available: the computational details for the benchmark boranes, along with their geometries and topologies are presented as supplementary information. See DOI: 10.1039/x0xx00000x

In an attempt to unravel the ambiguity concerning the bonding in **1** and how it influences the interactions that stabilise the

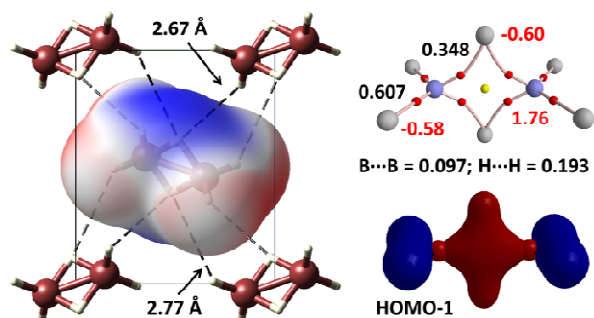


Fig. 1 Plot of the electrostatic potential superimposed on a 0.001 au isodensity surface ranging from -0.01 au (red) to 0.03 au (blue) of **1** viewed along the bc plane of the crystal. These calculations were constrained by the experimental X-ray diffraction data using a technique known as “wavefunction fitting”. Molecular graph displaying the bond and ring critical points as red and yellow spheres, along with the atomic charges and selected δ values in red and black. Plot of the HOMO-1 for **1** with isoelectronic density levels of ± 0.10 au.

extended structure of this borane, we carried out a topological analysis of the electron distribution for an isolated B_2H_6 molecule, using the concepts espoused in the quantum theory of “Atoms in Molecules” (AIM).⁹ This approach revealed a substantial amount of density ($\rho_b(r) = 1.67 \text{ e}\text{\AA}^{-3}$) evenly distributed throughout the B-H-B framework, albeit skewed towards the midpoint of the $B(\mu\text{-H})_2B$ moiety.¹⁰ Furthermore, the Laplacian of the electron density, $L(r) = -\nabla^2\rho(r)$, shows that the bridging hydrogen atoms are defined by local regions of charge concentration, indicating that each hydrogen atom is negatively charged. The positive electrostatic potential observed in the vicinity of the bridging hydrogen atoms results from an asymmetric distribution of density as the charge is redirected towards the boron atoms, leaving the hydrogen outwardly depleted. This shift of density towards the midpoint of the $B(\mu\text{-H})_2B$ moiety gives rise to highly polarised hydrides, with the regions of charge depletion directed towards the neighbouring molecules, allowing the B_2H_6 moieties to engage in what are best described as weak heteropolar hydride-hydride interactions to stabilise the solid-state structure.

The delocalisation index, $\delta(A,B)$, provides an alternative means of interpreting the bonding in **1**, since this parameter measures the number of electrons shared between two atoms.¹¹ In this instance, the large δ values calculated for the bridging B-H moieties show that a certain degree of covalent character is retained upon establishing the 3c,2e bonding, with $\sim 57\%$ of the density located in their terminal B-H counterparts (Fig. 1). Interestingly, the accretion of electron density at the midpoint of the $B(\mu\text{-H})_2B$ moiety also results in small δ values for the $B\cdots B$ and $H\cdots H$ contacts. Such a scenario is reflected in the HOMO-1 of this system, in which favourable overlap of boron 2p-orbitals is accompanied by an interaction with the 1s-orbitals of the bridging hydrogen atoms (Fig. 1). These findings support the previous diamond-shaped description of **1**, in which the density of the bridging hydrogen

atoms is polarised towards the $H_2B\cdots BH_2$ bond, again accounting for the reversal in polarity of these hydrides.¹²

The proclivity of boranes and related molecules to engage in

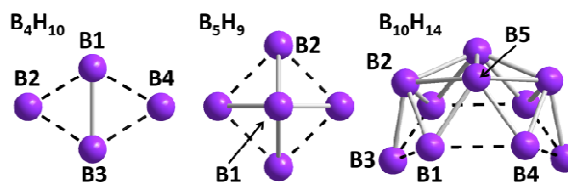


Fig. 2 Plot of the core structures for **2-4**, including labels for select boron atoms. The hydrogen atoms are omitted for clarity.

$B\cdots H\cdots B$ interactions is further revealed from a statistical survey of the Cambridge Structural Database (CSD), which returns over 1,600 structures containing $H\cdots H$ contacts between 2.0 and 2.8 Å. This led us to extend our analysis of hydride-hydride bonding to tetraborane-10 (B_4H_{10} - **2**), pentaborane-9 (B_5H_9 - **3**), and decaborane-14 ($B_{10}H_{14}$ - **4**), since these compounds are capable of forming a diverse array of $H\cdots H$ interactions (Fig. 2). This survey has afforded a clearer understanding of how variations in the size and shape of these clusters influence their choice of weak interactions.

The prototypical arachno-borane B_4H_{10} , **2** crystallises in the monoclinic space group $P2_1/n$ (#14), in which the asymmetric 3c,2e bonding was considered by Förster et al. to be described most appropriately as a central $B_2H_6^{2-}$ component interacting with two BH_2^+ fragments.¹³ This study showed that the interaction between the bridging hydrogen atoms and the peripheral BH_2^+ groups are around one-third weaker than their shorter B-H-B counterparts attached directly to the $B_2H_6^{2-}$ moiety (*i.e.* B1-H \cdots B2). Nevertheless, these interactions still accumulate half the density observed in their terminal counterparts. Förster et al. found no evidence of any $B\cdots B$ interactions between the $B_2H_6^{2-}$ and BH_2^+ fragments, supporting the partitioned model described above.¹³ This is consistent with our calculations for B_4H_{10} , with the exception of weak $B\cdots B$ interactions between the $B_2H_6^{2-}$ and BH_2^+ fragments as revealed by their small δ values (Fig. 3). $\nabla^2\rho(r)$ plotted in the plane of the 3c,2e B-B-B and B-H-B bonding clearly shows that the density is highly localised along the activated B-H bonds of the $B_2H_6^{2-}$ component, while being polarised towards the boron atoms of the BH_2^+ fragments (Fig. S4). The resulting electrostatic potential plotted on a 0.001 au isodensity surface for **2** reveals that the bridging hydrogen atoms are again electrophilic, allowing them to engage in weak heteropolar dihydrogen bonds with the terminal B-H groups.

The positive electrostatic potential in **2** is comparable in

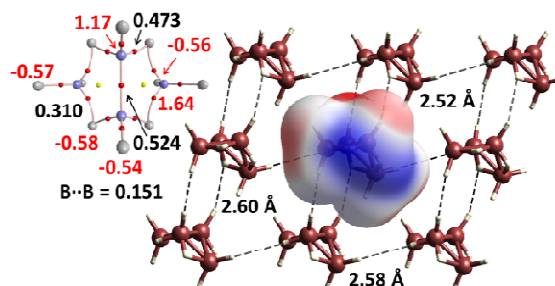


Fig. 3 Molecular graph of **2** displaying bond and ring critical points as red and yellow spheres, with atomic charges and selected δ

values in red and black. Plot of the electrostatic potential superimposed on a 0.001 au isodensity surface ranging from -0.01 au (red) to 0.03 au (blue) viewed along the ac plane of the crystal.

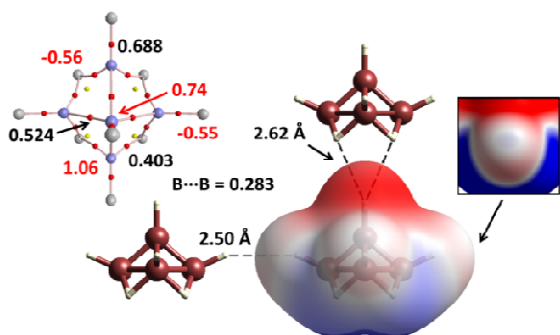


Fig. 4 Molecular graph of **3** displaying bond and ring critical points as red and yellow spheres, with atomic charges and selected δ values in red and black. Plot of the electrostatic potential superimposed on a 0.001 au isodensity surface ranging from -0.02 au (red) to 0.05 au (blue) viewed along the ac plane of the crystal. The insert shows the electrostatic potential for a terminal B-H bond with values ranging from -0.01 to 0.01 au.

magnitude with that calculated for **1**, but its size and shape allows the B_4H_{10} molecules to form slightly stronger H...H interactions (≥ 2.58 Å). In this instance, the terminal B-H bonds of the $B_2H_6^{2-}$ fragment interact with the bridging hydrogen atoms of a neighbouring molecule, to extend the structure in a zig-zag orientation along the a-axis of the crystal. This geometry also results in the close approach of two terminal B-H groups (2.52 Å), one defined by a negative region of electrostatic potential and the other by a small positive potential that carries over from the bridging hydrogen atoms. The remaining dimensions of the solid are then stabilised by heteropolar dihydrogen bonding involving the BH_2^+ moieties, confirming that the condensed phase of this borane is held together exclusively through attractive H...H interactions.

The molecular structure of the simple nido-borane B_5H_9 , **3** consists of a square pyramidal arrangement of the B-H moieties, with bridging hydrogen atoms connecting each of the basal boron atoms (Fig. 4).¹⁴ The symmetric 3c,2e bonding closely resembles the structural motif observed in **1**, albeit with slightly less density distributed throughout the B-H-B moieties, $\rho_b(r) = 1.61 \text{ eÅ}^{-3}$. Nevertheless, the δ values calculated for the equatorial B...B contacts signifies a moderate interaction between these atoms, with values nearly three times greater than their counterpart in **1**. Indeed, these B2...B2 interactions share approximately half the electron density present in the established B1-B2 bonds, whereas the related B-B-B bonding in **2** is more localised on the $B_2H_6^{2-}$ fragment. In addition, a plot of $\nabla^2\rho(r)$ in the plane of the equatorial boron atoms shows that the B...B interactions are defined by local regions of charge concentration (Fig. S6), similar to the hybrid bonding described in **1c**. This delocalisation results in additional skeletal electrons for the square-pyramidal framework, and highly polarised bridging B-H-B moieties that give rise to an electron-deficient region directly below the basal plane of this molecule.

The body-centred orientation of the B_5H_9 moieties in **3** allows the negative region of electrostatic potential surrounding the axial

B-H bond to interact with the electrophilic bridging hydrogen atoms of a neighbouring molecule, extending the structure of this borane along the c-axis of the crystal. However, the multifurcated nature of

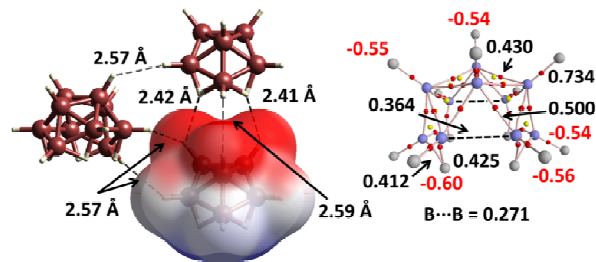


Fig. 5 Molecular graph of **4** displaying bond and ring critical points as red and yellow spheres, with selected atomic charges and δ values in red and black. Plot of the electrostatic potential superimposed on a 0.001 au isodensity surface ranging from -0.02 au (red) to 0.07 au (blue).

these dihydrogen bonds leads to longer than expected H...H contacts (2.62 Å), in spite of more favourable electrostatic interactions. The remaining dimensions of the solid are then stabilised through homopolar dihydrogen bonding between the equatorial B-H bonds. These hydride-hydride interactions are able to overcome the electrostatic repulsion imposed by the close proximity of two hydrides by forming σ -holes (*i.e.* positive or neutral regions of electrostatic potential at the apex of the covalent B-H bonds; Fig. 4). This subtle change in the charge distribution of **3** minimises the electrostatic repulsion in this region of the molecule, allowing for the formation of weak H...H interactions (2.50 Å). It is noteworthy that this type of behaviour is also observed in systems that exhibit halogen bonding, which also involve a strong interaction between two negatively charged atoms.¹⁵

The nido cluster B_4H_{10} , **4** adopts a capped arrangement of the skeletal B-B-B framework, with asymmetric 3c,2e B-H-B bonding at the open face of this structure. However, a recent topological analysis of the electron distribution in **4** by Kononova et al. proposed instead a structure that consists of two interconnected B_6 sub-clusters, since only a single mutual B-B bond was observed between the edges of these moieties.¹⁶ In contrast, our analysis of the δ values for the B1...B4 contacts in **4** revealed moderately strong interactions that effectively close the cage-like structure of this borane (Fig. 5). These values show that the B1...B4 interactions share only slightly less electron density than the strongest B-B bond of this cluster (>70%). Nevertheless, a plot of $\nabla^2\rho(r)$ in the B1-B5-B4 plane of **4** reveals charge concentrations between the B1-B5 and B4-B5 bonds, with the density being shifted inwards and away from the longer B1...B4 interactions (Fig. S8). In a similar vein, the B...B contacts within the B-H-B moieties also display moderate δ values, with the electron density of the bridging hydrogen atoms being polarised towards the midpoint of these B...B interactions, analogous to the 3c,2e bonding found in the structure of **3**.

The highly delocalised distribution of density in **4** results in an electrophilic region located at the open rim of this nido structure (Fig. 5). This behaviour is analogous to its smaller nido congener **3**, although the increase in Lewis acidity of the bridging hydrogen atoms in **4** gives rise to considerably stronger bifurcated H...H interactions (≥ 2.41 Å). This bonding motif extends the structure of **4**

along the c-axis of the crystal, with the remaining dimensions of the solid being held together by weaker heteropolar hydride-hydride bonding. Accordingly, the H...H contacts in **4** involve only an

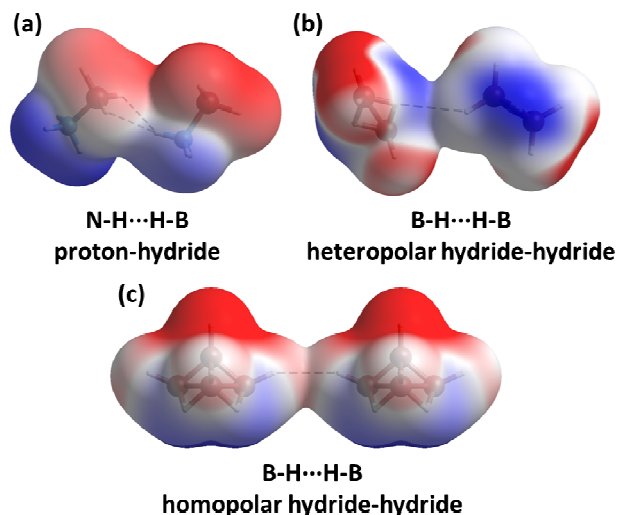


Fig. 6 Plot of the electrostatic potential superimposed on a 0.001 au isodensity surface for archetypal proton-hydride (NH_3BH_3), heteropolar hydride-hydride (B_2H_6), and homopolar hydride-hydride (B_5H_9) interactions.

interaction between positive and negative regions of the $\text{B}_{10}\text{H}_{14}$ molecules, whereas the smaller size of **3** forces the basal B-H groups in B_5H_9 to engage in secondary homopolar dihydrogen bonding.

In summary, this study has revealed the remarkably variable nature of the hydride moieties in the simple binary boranes **1-4**, which results in a rich spectrum of intermolecular H...H interactions that serve to stabilise their crystalline phases. In contrast to the electron-precise terminal B-H bonds in which the density is polarised towards the hydrogen atom, the density in their 3c,2e B-H-B counterparts accretes in the vicinity of the boron atoms, making the bridging hydrogen atoms comparatively Lewis acidic. Moreover, the 3c,2e B-H-B moieties experience only a marginal increase in electron density on going from **1-4**, whereas the charge that accumulates in the 3c,2e B-B-B skeletal bonds increases more rapidly. This effect serves to accentuate the relative Lewis acidity of the B-H-B hydrides, inviting an interaction with the basic terminal B-H moieties of a neighbouring molecule. Finally, this analysis of the electronic and supramolecular structures of **1-4** has revealed a previously unappreciated type of heteropolar hydride-hydride interaction on the spectrum of this neophyte class of dihydrogen bonding, which in some respects resembles more conventional N-H...H-B proton-hydride interactions (Fig. 6), in contrast to their homopolar B-H...H-B counterparts that involve a primary repulsive electrostatic interaction that is transcended by attractive dispersion forces.⁶

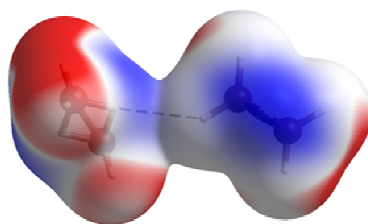
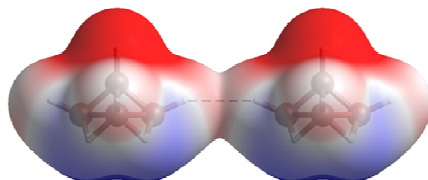
Notes and references

† The calculated electrostatic potentials discussed throughout this manuscript involve structures in good agreement with the geometries reported for their experimental models, with the

exception of the terminal B-H moieties which are fixed to neutron diffraction values of related bonds (1.180 Å).

‡ We are grateful to the Natural Sciences and Engineering Research Council of Canada and the ACENET consortium of Compute Canada for support of this work.

- 1 A. Stock, *Hydrides of Boron and Silicon*, Cornell University Press, Ithaca, NY, 1933.
- 2 K.S. Pitzer, *J. Amer. Chem. Soc.*, 1945, **67**, 1126-1132.
- 3 R.A. Ogg, *J. Chem. Phys.*, 1954, **22**, 1933-1935.
- 4 a) H.C. Longuet-Higgins and R.P. Bell, *J. Chem. Soc.*, 1943, 250-255; b) R. Hoffman and W.N. Lipscomb, *J. Chem. Phys.*, 1962, **37**, 2872-2883.
- 5 R.S. Lobayan, R.C. Bochicchio, A. Torre and L. Lain, *J. Chem. Theory Comput.*, 2009, **5**, 2030-2043.
- 6 a) D.J. Wolstenholme, J.T. Titah, F.N. Che, K.T. Traboulee, J. Flogeras and G.S. McGrady, *J. Am. Chem. Soc.*, 2011, **133**, 16598-16604; b) P. Sirsch, F.N. Che, J.T. Titah and G.S. McGrady, *Chem. Eur. J.*, 2012, **18**, 9476-9480; c) D.J. Wolstenholme, K.T. Traboulee, Y. Hua, L.A. Calhoun and G.S. McGrady, *Chem. Commun.*, 2012, **48**, 2597-2599; d) D.J. Wolstenholme, J. Flogeras, F.N. Che, A. Decken and G.S. McGrady, *J. Am. Chem. Soc.*, 2013, **135**, 2439-2442; e) D.J. Wolstenholme, J.L. Dobson and G.S. McGrady, *Dalton Trans.*, 2015, **44**, 9718-9731; f) D.J. Wolstenholme, M.M.D. Roy, M.E. Thomas and G.S. McGrady, *Chem. Commun.*, 2014, **50**, 3820-3823.
- 7 H.W. Smith and W.N. Lipscomb, *J. Chem. Phys.*, 1965, **43**, 1060-1064.
- 8 a) A. Zabardasti, A. Kakanejadifard, A.-A. Hoseini and M. Solimannejad, *Dalton Trans.*, 2010, **39**, 5918-5922; b) A. Zabardasti, M. Joshaghani, S. Nadri, H. Goudarziashar and M. Salehanaddaj, *Struct. Chem.*, 2012, **23**, 1497-1502.
- 9 R.F.W. Bader, *Atoms in Molecules: A Quantum Theory*, Oxford University Press, Oxford, U.K., 1990.
- 10 C.B. Hübschle, M. Messerschmidt, D. Lentz and P. Luger, *Z. Anorg. Allg. Chem.*, 2004, **630**, 1313-1316.
- 11 X. Fradera, M.A. Austen and R.F.W. Bader, *J. Phys. Chem. A*, 1999, **103**, 304-314.
- 12 F. Wang, W. Pang and M. Huang, *J. Electron Spectrosc. Relat. Phenom.*, 2006, **151**, 215-223.
- 13 D. Förster, C.B. Hübschle, P. Luger, T. Hügler and D. Lentz, *Inorg. Chem.*, 2008, **47**, 1874-1876.
- 14 W.J. Dulmage and W.N. Lipscomb, *Acta Cryst.*, 1954, **5**, 260-264.
- 15 P. Politzer, P. Lane, M.C. Concha, Y. Ma and J.S. Murray, *J. Mol. Model.*, 2007, **13**, 305-311.
- 16 E.G. Kononova and Z.S. Klemenkova, *J. Mol. Struct.*, 2013, **1036**, 311-317.

Graphical Abstract:**Heteropolar Hydride-Hydride****Homopolar Hydride-Hydride**

The nature and driving forces behind the formation of dihydrogen bonds are explored in several textbook boranes, and their influence on the crystalline architecture is revealed.